Open Access

Original Article

Estimation of Critical Sized Bone Defect for Biomaterial Implantation and Evaluation of Newly Formed Bone by Quantitative Histomorphometry, using Silicon Substituted Hydroxyapatite for Bone Tissue Engineering Purpose

Muhammad Marghoob Khan, Shadab Ahmed Butt*, Aqif Anwar Chaudhry, Abdullah Qamar, Ayesha Ali***, Mahjabeen Fatima**

Department of Anatomy, Army Medical College/National University of Medical Sciences (NUMS) Rawalpindi Pakistan, *Department of Anatomy, Akther Saeed Medical College, Rawalpindi Pakistan, **Department of Biomaterials, COMSATS University Islamabad, Lahore Campus Pakistan, ***Department of Anatomy, Foundation University Medical College, Rawalpindi Pakistan

ABSTRACT

***Objective*:** To determine Critical sized bone defect in Rabbit tibiae for evaluation of implanted biomaterial and to quantify new bone formation to see the osteogenic effect of Silicon substituted Hydroxyapatite.
***Study Design*:** Lab-based experimental study.
***Place and Duration of Study*:** Anatomy Department, Army Medical College, Rawalpindi Pakistan, from Aug 2021 to Jan 2023.
***Methodology*:** A total of 30 New Zealand White rabbits, divided into six Groups (n=5) were used. After Anesthesia, a bone defect measuring 6 x 6 x 6mm was drilled in the right tibiae in Group A1 and A2 (sacrificed after 4 and 6 weeks, respectively) and 9 x 6 x 6mm in Group A3 (sacrificed after 6 weeks). Silicon hydroxyapatite, alone with stromal vascular fraction, was placed in Experimental Groups II, III, and IV.
***Results*:** All rabbits in Group A3 showed no defect closure, indicating that it was a critical-sized defect. The median values with interquartile ranges (IQR) of p=0.004 among the Groups indicated that Group IV had a significantly increased total bone area compared to the other Groups. In Group comparisons, no statistical difference was observed between Group I and II, Group II and III, or Group II and IV. However, a statistically significant difference was observed between Group I and IV (p-value =0.002).
***Conclusion*:** A defect size of 9 x 6 x 6 mm may be suitable for studies of shorter duration, and bone area quantification can be used to assess new bone formation.

Keywords: Bone, Bone Regeneration, Histology, Hydroxyapatites, Stromal Vascular Fraction, Tissue Engineering.

How to Cite This Article: *Khan MM, Butt SA, Chaudhry AA, Qamar A, Ali A, Fatima M. Estimation of Critical Sized Bone Defect for Biomaterial Implantation and Evaluation of Newly Formed Bone by Quantitative Histomorphometry, using Silicon Substituted Hydroxyapatite for Bone Tissue Engineering Purpose. Pak Armed Forces Med J 2025; 75(3): 501-507. DOI: https://doi.org/10.51253/pafmj.v75i3.12885*

INTRODUCTION

Bony lesions and defects are usually attributed to old age, inflammation, trauma, tumors, etc.[1] Some of these defects, measuring 2cm or more or surpassing 50% of the defect circumference, are classified as Critical bone defects (CSDs), which are not capable of complete regeneration. Recent research on biomaterials development for restoring such defects has proven to be effective.[2] One of the most widely used biomaterials for bone tissue engineering (BTE) is Hydroxyapatite (HAP), often written as Ca10 (PO4)6(OH)2, a calcium phosphate-based material having similarities to the human bone.[3] Due to its biocompatibility and bioactivity, HAP is applied in bone and dental applications. HAP is synthesized using diverse methods, such as the sol-gel process, wet chemical precipitation, and hydrothermal synthesis, each with its own set of advantages and disadvantages.[4] Synthetic bone substitutes have lately been modified with trace elements, e.g., Silicon (Si), strontium (St), magnesium iron, etc., to improve their therapeutic effects.[5] Silicon-substituted hydroxyapatite (Si-HA) has been found to enhance bioactivity *in vivo* as compared to HA, having beneficial effects on bone formation.[6]

In evaluating a material for bone regeneration, a biomaterial can only be considered an effective alternative if it can enhance the healing capacity of CSD. CSDs can be defined as a defect that, during the lifespan of a specific animal model, results in bone regeneration of less than 10% or, if left untreated, fails to heal within a specific time frame.[7] American Society for Testing and Materials (ASTM) Standard Guide for Preclinical *in vivo* Evaluation on Critical Size Segmental Bone Defects (F2721-09) defines it as "a defect that will not heal spontaneously without intervention within the lifetime of animal or experiment."[8] Nevertheless, not only different animal species have different regenerative potentials but also

Correspondence: Dr Muhammad Marghoob Khan, Department of Anatomy, Army Medical College, Rawalpindi Pakistan
Received: 18 Nov 2024; revision received: 19 Mar 2025; accepted: 18 Apr 2025

even in same species of animals, there are differences in CSDs created in the same region, posing limitations.[7] Various CSDs in different anatomical regions in different animal models are being used for research purposes, such as the long bones, the skull, the alveolar bone, etc.[9]

Establishing a CSD in an animal model is considered a crucial step for *in vivo* studies for biomaterial compatibility. Since the size of a CSD in the rabbit model is a matter of debate, with various authors proposing different sizes, we propose a hypothesis that if the depth and width are determined, the length of the CSD should be between 8 and 10 mm for a study duration spanning 6 to 7 weeks. This study aimed to determine a suitable size of CSDs for biomaterial implantation with a shorter duration and to evaluate the amount of regenerated bone using quantitative histomorphometry, utilizing Si-HA and autologous adipose tissue-derived stromal vascular fraction (SVF) for BTE purposes.

METHODOLOGY

The study was conducted at the Anatomy Department, Army Medical College, Rawalpindi; the National Institute of Health, Islamabad (NIH); and the Interdisciplinary Research Center for Biomedical Materials (IRCBM), COMSATS University, Islamabad (CUI), Lahore campus, Pakistan. The study was conducted in the laboratory from August 2021 to January 2023. After approval from the Ethical Review Committee of Army Medical College, Rawalpindi (ERC, AMC). Ethics approval was obtained from the Institutional Animal Care and Research Committee of Army Medical College in accordance with the Animal Research: Reporting of In Vivo Experiments (ARRIVE) guidelines. All methods were performed in compliance with the relevant guidelines and regulations. 30 New Zealand White rabbits were divided into six Groups (n=5), out of which Groups A1, A2 and A3 were used to ascertain CSD. In contrast, experimental Groups II, III, and IV were used for the evaluation of Si-HA by histomorphometry.

Inclusion Criteria: Healthy, adult female New Zealand White rabbits with an average weight between 1700 and 2500 grams were used.

Exclusion Criteria: Adult male rabbits, adult pregnant female rabbits, and rabbits already on drug therapy, used in any other study/experiment within the last month, or on medication for any disease in the past month were excluded.

For creating bone defect, rabbits were anesthetized with intramuscular injection of Xylacine 5mg/kg (Xylax® 2%, 25mL) and Ketamine 35mg/kg (Ketolar® 50mg/mL) and operated upon as before.[10] After disinfection with 10% povidone-iodine, an incision was given on the medial side of the tibia of the right leg. Using a surgical drill (Escort-III Micromotor, Saeyang Marathon, H20, South Korea) with saline irrigation, a bone defect measuring 6mm in length x 6mm in breadth and 6mm in depth was drilled in the right tibiae of each rabbit of Group A1 and Group A2, and a defect measuring 9mm x 6mm x 6mm was drilled in Group A3. The depth and size of the defect were measured with the help of a metal wire positioner with mm markings. Rabbits in Group A1 were sacrificed after 4 weeks, while rabbits in Group A2 and A3 were sacrificed after 6 weeks. The bones of each Group were examined, and after ascertaining the defect in Group A3 as critical-sized (renamed as Group I, to be used as a control Group), a defect measuring 9mm x 6mm x 6mm was drilled in tibiae of rabbits of experimental Group II, III and IV. Adipose tissue for SVF was dissected from the rabbits in the right inguinal region, and SVF (enzymatic and modified non-enzymatic) was isolated as before.[11] Si-HA alone was implanted in Group II, while Si-HA along with SVF-derived enzymatically and non-enzymatically modified were placed in Experimental Groups III and IV, respectively.[12,13] Wound closure was performed using metallic staples, which were removed 10 days postoperatively. Euthanizing of rabbits was carried out after a designated time interval, following which tibiae were dissected for gross morphologic and histologic observations.[8]

For bone histomorphometry, from each specimen of control and experimental Groups, two consecutive 5-µm sections along the longitudinal plane were obtained and, after processing with alcohol and xylene (70%, 90%, and 100%), were stained with Hematoxylin and Eosin (H&E) as per manufacturer's instructions. Analysis and photography of the sections were performed using a microscope (Olympus-CX41, Olympus, Japan) connected to a CCD camera (DP72; Olympus, Japan) and CellSens software (Olympus, Japan). Sections were analyzed with standard histomorphometric techniques at 10× in the center of the defect, and area and percentage new bone formation calculated as follows: Using different colors to outline different parameters, a 7 × 7 cm square overlapping the center of the defect was obtained at 10× magnification for estimate percentages of bone (B),

bone marrow (BM), Connective tissue (CT), and the residual spaces (RS) left by remaining biomaterial in the region of interest (Total area) (Figure-1). The total bone area was calculated by subtracting bone marrow (BM), Connective tissue (CT), and the residual spaces from the total area (region of interest, ROI) scanned, and the percentages of residual spaces, BM%, bone tissue%, and CT% were calculated as follows for each slide as follows:

Residual spaces% = RS × 100/ROI (Region of interest/total area)

Connective tissue% = CT × 100/ROI

BM% = BM × 100/ROI

Bone tissue% = MB × 100/ROI

The CT scan included both fibrous tissue and blood vessels.[14]

The percentage of new bone formation and defect area closure was calculated from the Median of each Group. Data were analyzed using the Kruskal-Wallis test and post hoc analysis with the Statistical Package for the Social Sciences (SPSS) version 20. Kolmogorov–Smirnov test and the Shapiro–Wilk test were applied to check the normality of the data. As the normality assumptions were not met, all quantitative variables were explored using the median and interquartile range (IQR), while frequencies and percentages were calculated for qualitative variables. The *p*-value of 0.05 or less was considered significant.

RESULTS

Observation of the surgical site after six weeks revealed a healed wound with no evidence of dehiscence or infection. After dissecting the tibia, all the bones were carefully cleared of connective tissue, with particular attention paid to the defect area, and then measured. The bones showed normal gross morphological features with no signs of infection or bone loss. All bones in Groups A1 and A2 showed indistinguishable defect margins and complete closure of the defect after 4 and 6 weeks, respectively, indicating a non-critical defect. In all bones of Group A3, the defect area was still visible, and the defect margins were distinguishable on naked-eye examination, confirming the size of the defect as being critical-sized. At the same time, Si-HA was still visible in varying amounts in the defect area of rabbits of Groups II, III, and IV (Figure-2d). One rabbit each from Group II (rabbit 2), Group III (rabbit 1), and Group IV (rabbit 1) did not exhibit Si-HA in the defect, which was also evident histologically. However, healing was more apparent in the treatment Group compared to the control Group, both in naked-eye examination and histologically. Histomorphometric analysis at 6 weeks revealed that the defect size remained largely unchanged, with minimal to no new bone formation in the defect center, as indicated by the presence of islands of bone in all rabbits of Group I (control) and no evidence of bone remodeling. The osseous activity was observed to be minimal, indicated by a thin layer of osteoid matrix lining the periphery of the defect (Figure- 1a).

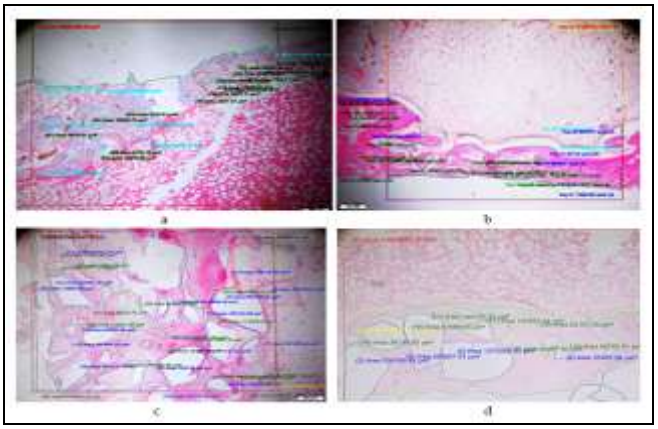

Figure-1: Histological Analysis for Area Measurement at 6 weeks; a: Group I, b: Group II, c: Group III and d: Group IV (magnified) (d), H & E (10X). Key: Red: Total area (7x7cm), Yellow: Bone Marrow, Blue: Residual Spaces (Empty Space in Slide and Area Occupied by the Biomaterial), Green: Connective tissue, Black: Area of the Defect Closed. Bar = 500 µm

In the experimental Groups, newly formed bone was observed in continuity with the bone present at the margin of the defects or in islands interspersed between the residual biomaterial spaces and the bone marrow (Figures-1b, c, and d). The amount of newly-formed bone in Group II (Si-HA only) 16.02±3.18%, Group III (Si-HA+SVF – Enzymatic isolation) 26.22±12.22% and Group IV (Si-HA+SVF – Non Enzymatic isolation) 34.59±6.28%, was significantly higher than that in the control Group I, 7.25±5.07% (Figure-3). The least amount of bone formed in Group II was 10.5% in rabbit no two and in Group III in rabbit no 5 in the center of the defect, while all rabbits in Group IV showed increased bone formation as compared to other Groups. In Group comparisons, no statistically significant difference was observed between the amounts of newly-formed bone in Group I and Group II (*p*-value =0.988), Group II and III (*p*-value =1.000), and Group II and IV (*p*-value =0.170). In contrast, a near-significant trend was observed between Groups I and III (*p*-value =0.053).

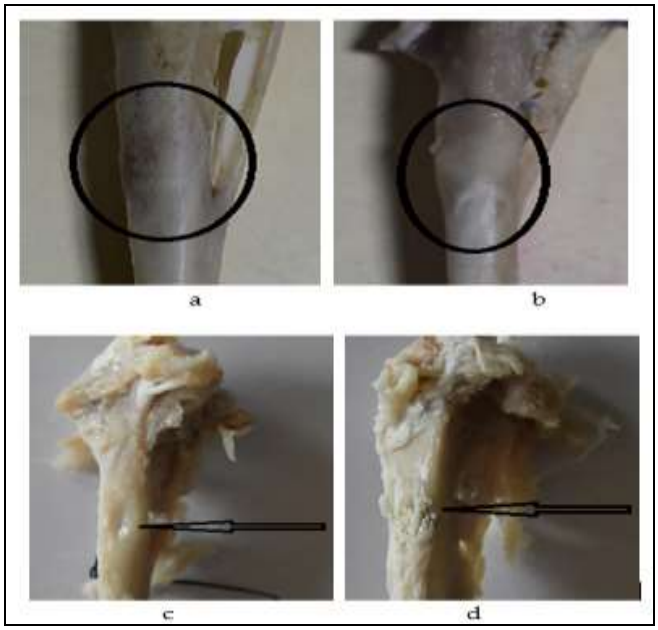

Figure -2: a; Healed Defect in Group A1 (Black circle), b; Healed Defect in Group A2 (Black circle), c; CSD in Group A3 with Clear Margins (Black Arrow), d; Defect Filled with Si-HA in Experimental Group II

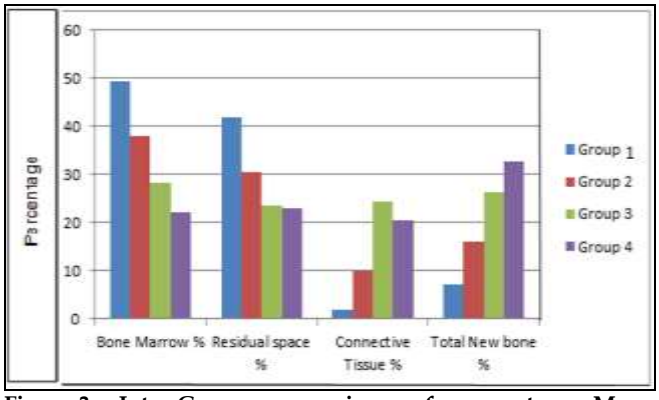

Figure-3: Inter-Group comparison of percentage Mean Grading Score of Bone marrow, Residual spaces, connective tissue and New bone

Table-I: Median, interquartile ranges (IQR) of Defect Area closed and Total Area New Bone Formation (n=20)

Parameters	Group-I (n=5) Median (IQR)	Group-II (n=5) Median (IQR)	Group-III (n=5) Median (IQR)	Group-IV (n=5) Median (IQR)	*p*-value
Total Bone Area (µm)	925908.40 (2020282.99)	4191307.90 (1100947.10)	5539813.88 (5758132.72)	7925563.46 (4098712.41)	0.002
Defect Area (µm)	0.00 (0.00)	6496132.38 (8126224.89)	12767830.59 (7732945.16)	11081108.97 14414540.88)	0.004

The median values with interquartile range (IQR) of *p*=0.004 among the Groups indicate that the addition of non-enzymatically derived SVF significantly increased total bone area compared to the untreated defect (Table-I). On the other hand, a statistically significant difference was observed between Groups I and IV (*p*-value =0.002) (Table-II). It was also evident histologically that, percentage-wise, both Group III and Group IV showed a greater amount of newly formed bone than the Si-HA-only Group (Figures 1 and 3).

Table-II: Inter-group Comparison of Area of the Defect Closed and Total Area New Bone Formation (n=20)

Group Comparison	Group-I Vs. Group-II	Group-II Vs. Group-III	Group-I Vs. Group-III	Group-II Vs. Group-IV	Group-I Vs. Group-IV	Group-III Vs. Group-IV
Total Bone Area (µm)	*p*=0.988	*p*=1.000	*p*=0.053	*p*=0.170	*p*=0.002	*p*=1.000
Bone Defect (µm)	*p*=0.402	*p*=0.789	*p*=0.005	*p*=1.000	*p*=0.022	*p*=1.000

DISCUSSION

Critical bone defects (CSDs) have been considered a significant obstacle for orthopedic surgeons due to bone loss or excision in cases of trauma, blast injuries, bone tumors, etc. Recent advancements to deal with CSDs include the concept of BTE, including a combination of natural or synthetic biomaterials, either alone or along with implanted stem cells or cytokines, etc.[10]

The rabbit model of bone defect for studies involving materials is an ideal alternative before being used in human trials. The rabbits not only exhibit basic multicellular unit remodeling and share a similar bone density compared to human counterparts but also have a cortical bone modulus and strength more similar to humans than to those of other animals. All these factors make rabbits more suitable as ideal models for BTE studies, particularly for shorter-duration studies.[15]

Researchers have utilized various CSD models of different sizes in rabbits to evaluate biomaterials in studies. In this context, a CSD model of 5mm × 10mm in right lateral femoral condyles by Sadek *et al.*,[10] a defect of 8mm × 3mm × 2mm in rabbit mandible by Wang *et al.*,[16] and a defect in the femur measuring 6mm x 8mm and a defect of 15mm created by Dasgupta *et al.*,[17] for their studies. It is pertinent to note that most of the defects used by these researchers were defined by only two parameters: length and breadth or length and depth. We suggest that to create a CSD, all three parameters—width, length, and depth — must be included to define the CSD clearly. For this reason, we used a defect model containing all these parameters for different experimental durations in all Groups. The absence of bone regeneration in both histological and gross morphological observations in

Group C1 at 6 weeks confirmed that the model used was a critical-size one (Figures 2c and 1a).

During the creation of a bone defect with an electric drill, thermal damage leading to bone necrosis can be caused by excessive drill speed, which increases bone absorption and cell degeneration. The bony tissue can tolerate a maximum temperature of 47°C for a period of one minute without causing permanent damage. On the other hand, lower temperatures facilitate bone regeneration, and for this reason, it is suggested to avoid thermal damage by using copious irrigation with saline while using a drill machine.[18] In our study, an electric drill with a controlled and constant speed was used while continuing irrigation with 0.9% normal saline. In the control Group and all experimental Groups, we noted bleeding during the procedure, with no evidence of a severe inflammatory reaction or cell necrosis afterward, suggesting that adequate thermal control with minimal interference to the experiment was achieved.

Considering the percentage of new bone formation in the defect area, a high percentage of newly formed bone was observed histologically in all three experimental Groups as compared to the control Group, which is in accordance with other studies. Borie et al. reported less bone formation in the control Group with 8mm defects compared to the study Groups.[19] In this regard, the highest percentage of new bone formation was evident in Group IV, followed by Group III, signifying the osteogenic potential of SVF. Better bone formation in Groups IV and III compared to Group II is most likely because different cell populations in the SVF cooperated and stimulated mesenchymal cell activity, confirming the interplay between stem cells and the microenvironment.[20,21] Roato *et al.,* compared the osteogenic potential of SVF in the presence of osteogenic factors with Adipose stromal cells (ASCs) alone and concluded that SVF has better osteoinductive capabilities than ASCs plated with the osteogenic medium.[22] The percentage of newly formed bone has been calculated by only a few authors, and most did not specify the exact methodology for calculating the bone area. However, some mentioned the use of computer software. A study conducted on rabbit calvaria, using nanocrystalline HA and human freeze-dried bone graft (FDGB), showed newly formed bone mean percentages in the NanoBone Group after 6 and 12 weeks as 21.57 and 23.86%, respectively, and for FDGB was 14.22% and 27.4% respectively.[23] In our study, we calculated the percentage of new bone formation by marking different areas in histological specimens and then manually calculating the percentage. In this context, Duan *et al.,* calculated the newly formed bone along with bone marrow. The authors used six commercially available CaP bone and two tricalcium phosphate (TCP) ceramics, which were implanted in the paraspinal muscles of four beagles. After 12 weeks, the percentage of new bone formation ranged from 0.1±0.1% to 21.6±4.5%, which is slightly more than in experimental Group II and significantly less than in experimental Groups III and IV of our study.[24] In another study, the percentage of new bone area was found to be 28.64±6.64% and 37.95±6.98% on the 14th day in implant Groups using strontium-incorporated micro/nano rough titanium surfaces in rats.[25] Similarly, histological evaluations showed newly formed bone as 73.33 and 48.91 in the antler xenograft and Cerabone Groups, which was significantly higher than the control 18.91.[23] The histomorphometric assessment of the above-mentioned studies is similar to our study, considering the pattern of new bone formation. The percentage of new bone formation in our experimental Groups was higher, and the above studies were performed using computer software without explicitly detailing the exact methodology for calculating percentages. In statistical analysis among Groups regarding new bone formation, no statistically significant difference was observed among Groups, except for a near-significant trend between Groups I and III (p=0.053) and a statistically significant difference between Groups I and IV (p=0.002). Similarly, for defect area closure, the median values with interquartile ranges (IQR) showed an increased closure of the defect by new bone from Group II, followed by Groups III and IV. A statistically significant difference (p=0.004) was observed among the Groups, further indicating the osteogenic capacity of Si-HA used in the current study. Considering lamellar and woven bone formation after 6 weeks, both were found in the experimental Groups. On the other hand, only woven bone was found in the control Group, indicating that the new bone formation and maturation in the control Group was significantly slower than in the experimental Groups. We found new bone dispersed as islands between the bone marrow and residual spaces, as well as in continuity with the older bone at the periphery of the defect, in all experimental Groups except the control. Hence, the absence of bone in the center of defects in the control Group and the presence of isolated bony islands in the

center of defects in the experimental Group can be attributed to the osteoconductivity of Si-HA.

It is better to calculate new bone without the addition of other components, such as bone marrow, as this will provide more precise values for the newly formed bone and a better understanding of the osteogenic qualities of the implanted material. This view is supported by the fact that we found a high percentage of bone marrow in the defect area, effectively closing the defect with very little newly formed bone. For instance, the bone marrow percentages in all rabbits of Group I are above 40% (Mean 49.36%), while the new bone formation was restricted to less than 13% (Mean 6.62%). On the other hand, rabbit number 3 of Group III has 6.8% bone marrow and 41% newly formed bone. Similarly, rabbit no. 2 of Group IV has 10.3% bone marrow and 41.83% newly formed bone. This, along with other readings from Groups III and IV, will significantly alter the mean percentage values of newly formed bone. A resultant comparison of newly formed bone along with bone marrow to other experimental Groups will give the control Group an added advantage, potentially giving the false impression of more new bone formation in the control Group compared to Groups II, III, and IV.

After placing a bone graft or biomaterial in a defect, it is essential to emphasize the quantity and quality of newly formed bone. Newly formed bone utilizing biomaterials has been studied using conventional qualitative studies. Although statistical analysis may not reveal significant differences in Group comparisons, percentages can provide an idea about the effectiveness of the implanted biomaterial. It is for this reason that we utilized a non-conventional in-depth analysis of bone by calculating the percentage of new bone. The goal is to utilize biomaterials for the treatment of CSDs and other bone diseases. With an increasing understanding of natural bone anatomy and histology, which facilitates an understanding of the bone regeneration process, a growing number of biomaterials are currently being investigated. Most in vivo histological results are based on the presence or absence of bone formation. An in-depth analysis, calculated as the percentage of new bone formation, clearly depicts differences between experimental Groups and can be used to assess new bone formation in studies involving biomaterials. Taking full advantage of Si-HA as a bone filler and utilizing SVF may be a component in the design of the next generation of orthopedic replacements.

CONCLUSION

During the creation of an elongated CSD, the inclusion of all three parameters, i.e., length, breadth, and width, clearly defines the extant CSD. Additionally, due to the non-healing of our defect in six weeks, a size of 9mm x 6mm x 6mm is feasible with a very low risk of complications. It may provide a clinically relevant foundation for future tissue engineering efforts in the tibia, supporting studies of shorter duration. Based on our results, Si-HA, when used alone or in combination with SVF, has the potential to be a promising material candidate for biomedical applications, exhibiting good bioactivity and mechanical properties that are essential for bone neoformation and filling bone defects.

Conflict of Interest: None.

Funding Source: None.

Authors' Contribution

Following authors have made substantial contributions to the manuscript as under:

MMK & SAB: Conception, study design, drafting the manuscript, approval of the final version to be published.

AAC & AQ: Data acquisition, data analysis, data interpretation, critical review, approval of the final version to be published.

AA & MF: Conception, data acquisition, drafting the manuscript, approval of the final version to be published.

Authors agree to be accountable for all aspects of the work in ensuring that questions related to the accuracy or integrity of any part of the work are appropriately investigated and resolved.

REFERENCES

1. Hellwinkel JE, Working ZM, Certain L, García AJ, Wenke JC, Bahney CS. The intersection of fracture healing and infection: Orthopaedics research society workshop 2021. J Orthopaed Res 2022; 40(3): 541-552. https://doi.org/10.1002/jor.25261
2. Nauth A, Schemitsch E, Norris B, Nollin Z, Watson JT. Critical-Size Bone Defects: Is There a Consensus for Diagnosis and Treatment? J Orthopaed Trauma 2018; 32 Suppl 1: S7-s11. https://doi.org/10.1097/BOT.0000000000001115
3. Shuai C, Peng B, Feng P, Yu L, Lai R, Min A. In situ synthesis of hydroxyapatite nanorods on graphene oxide nanosheets and their reinforcement in biopolymer scaffold. J Advan Res 2022; 35: 13-24. https://doi.org/10.1016/j.jare.2021.03.009
4. Fiume E, Magnaterra G, Rahdar A, Verné E, Baino F. Hydroxyapatite for Biomedical Applications: A Short Overview. Ceramics 2021; 4(4): 542-563.
5. Yang L, Ullah I, Yu K, Zhang W, Zhou J, Sun T, et al. Bioactive Sr(2+)/Fe(3+)co-substituted hydroxyapatite in cryogenically 3D printed porous scaffolds for bone tissue engineering. Biofabrication 2021; 13(3). https://doi.org/10.1088/1758-5090/abcf8d
6. Radulescu DE, Vasile OR, Andronescu E, Ficai A. Latest Research of Doped Hydroxyapatite for Bone Tissue Engineering. Int J Mole Sci 2023; 24(17). https://doi.org/10.1002/jbm.a.31549

7. Bodde EW, Spauwen PH, Mikos AG, Jansen JA. Closing capacity of segmental radius defects in rabbits. J Biomed Mater Res 2008; 85(1): 206-217. https://doi.org/10.1002/jbm.a.31549
8. Seman CNZC, Zakaria Z, Sharifudin MA, Ahmad AC, Awang MS, Yusof NM, et al. Model of A Critical Size Defect in the New Zealand White Rabbit's Tibia. IIUM Med J Malaysia 2018; 17(1). https://doi.org/10.31436/imjm.v17i1.305
9. Kengelbach-Weigand A, Thielen C, Bäuerle T, Götzl R, Gerber T, Körner C, et al. Personalized medicine for reconstruction of critical-size bone defects - a translational approach with customizable vascularized bone tissue. NPJ Regen Med 2021; 6(1): 49. https://doi.org/10.1038/s41536-021-00158-8
10. Sadek AA, Abd-Elkareem M, Abdelhamid HN, Moustafa S, Hussein K. Repair of critical-sized bone defects in rabbit femurs using graphitic carbon nitride (g-C3N4) and graphene oxide (GO) nanomaterials. Sci Rep 2023; 13(1): 5404. https://doi.org/10.31436/imjm.v17i1.305
11. Tiryaki T, Cohen SR, Canikyan Turkay S, Kocak P, Sterodimas A, Schlaudraff KU, et al. Hybrid Stromal Vascular Fraction (Hybrid-SVF): A New Paradigm in Mechanical Regenerative Cell Processing. Plastic Reconstruct Surg Global Open 2022; 10(12): e4702. https://doi.org/10.1097/GOX.0000000000004702
12. Asif A, Nazir R, Riaz T, Ashraf N, Zahid S, Shahid R, et al. Influence of processing parameters and solid concentration on microstructural properties of gel-casted porous hydroxyapatite. J Porous Mat 2014; 21(1): 31-37. https://doi.org/1 10.1007/s10934-013-9743-x
13. Blanco JF, García-Briñon J, Benito-Garzón L, Pescador D, Muntión S, Sánchez-Guijo F. Human bone marrow mesenchymal stromal cells promote bone regeneration in a xenogeneic rabbit model: a preclinical study. Stem Cells Int 2018; 2018. https://doi.org/10.1155/2018/7089484
14. Duan R, Barbieri D, De Groot F, De Bruijn JD, Yuan H. Modulating bone regeneration in rabbit condyle defects with three surface-structured tricalcium phosphate ceramics. ACS Biomat Sci Eng 2018; 4(9): 3347-3355. https://doi.org/10.1021/acsbiomaterials.8b00630
15. Mukherjee P, Roy S, Ghosh D, Nandi SK. Role of animal models in biomedical research: a review. Lab Animal Res 2022; 38(1): 18.
16. Wang Y, Zhang X, Mei S, Li Y, Khan AA, Guan S, et al. Determination of critical-sized defect of mandible in a rabbit model: Micro-computed tomography, and histological evaluation. Heliyon 2023; 9(7): e18047. https://doi.org/10.1016/j.heliyon.2023.e18047
17. Dasgupta S, Maji K, Nandi SK. Investigating the mechanical, physiochemical and osteogenic properties in gelatin-chitosan-bioactive nanoceramic composite scaffolds for bone tissue regeneration: In vitro and in vivo. Mat Sci Eng 2019; 94: 713-728. https://doi.org/10.1016/j.msec.2018.10.022
18. Togni F, Baras F, Ribas MdO, Taha MO. Histomorphometric analysis of bone tissue repair in rabbits after insertion of titanium screws under different torque. Acta Cirurgica Brasil 2011; 26: 261-266.
19. Souza EQM, Costa Klaus AE, Espósito Santos BF, Carvalho da Costa M, Ervolino E, Coelho de Lima D, et al. Evaluations of hydroxyapatite and bioactive glass in the repair of critical size bone defects in rat calvaria. J Oral Bio Craniofacial Res 2020; 10(4): 422-429. https://doi.org/10.1590/s0102-86502011000400003
20. Baer PC, Geiger H. Adipose-derived mesenchymal stromal/stem cells: tissue localization, characterization, and heterogeneity. Stem cells Int 2012; 2012. https://doi.org/10.1155/2012/812693
21. Später T, Frueh FS, Nickels RM, Menger MD, Laschke MW. Prevascularization of collagen-glycosaminoglycan scaffolds: stromal vascular fraction versus adipose tissue-derived microvascular fragments. J Bio Eng 2018; 12(1):1-13. https://doi.org/10.1186/s13036-018-0118-3
22. Roato I, Belisario DC, Compagno M, Verderio L, Sighinolfi A, Mussano F, et al. Adipose-derived stromal vascular fraction/xenohybrid bone scaffold: An alternative source for bone regeneration. Stem cells International. 2018; 2018. https://doi.org/10.1155/2018/4126379
23. Sargolzaie N, Kadkhodazadeh M, Ebadian AR, Shafieian R, Pourkaveh S, Naghibi N, et al. Histological Evaluation of Bone Regeneration Using Hydroxyapatite Based Bone Substitute Derived from Antler: An Animal Study. J Long-Term Eff Med Implants 2022; 32(1): 77-84. https://doi.org/ 10.1615/JLongTermEffMedImplants.2021039830
24. Duan R, Barbieri D, de Groot F, de Bruijn JD, Yuan H. Modulating Bone Regeneration in Rabbit Condyle Defects with Three Surface-Structured Tricalcium Phosphate Ceramics. ACS Biomat Sci Eng 2018; 4(9): 3347-3355. https://doi.org/10.1021/acsbiomaterials.8b00630
25. Xu T, Xu M, Lu Y, Zhang W, Sun J, Zeng R, et al. A trail pheromone mediates the mutualism between ants and aphids. Curr Bio 2021; 31(21): 4738-47.e4. https://doi.org/10.1016/j.colsurfb.2021.111992